

# Temporal and rate representations of time-varying signals in the auditory cortex of awake primates

Thomas Lu<sup>1</sup>, Li Liang<sup>1,2</sup> and Xiaoqin Wang<sup>1</sup>

<sup>1</sup> *Laboratory of Auditory Neurophysiology, Department of Biomedical Engineering, The Johns Hopkins University School of Medicine, 720 Rutland Avenue, Ross 424, Baltimore, Maryland 21205, USA*

<sup>2</sup> *Hearing Center, Pear River Hospital of First Medical University, Guangzhou 510282, Guangdong Province, P. R. China*

Correspondence should be addressed to X.W. ([xwang@bme.jhu.edu](mailto:xwang@bme.jhu.edu))

Published online: 9 October 2001, DOI: 10.1038/nn737

Because auditory cortical neurons have limited stimulus-synchronized responses, cortical representations of more rapidly occurring but still perceivable stimuli remain unclear. Here we show that there are two largely distinct populations of neurons in the auditory cortex of awake primates: one with stimulus-synchronized discharges that, with a temporal code, explicitly represented slowly occurring sound sequences and the other with non-stimulus-synchronized discharges that, with a rate code, implicitly represented rapidly occurring events. Furthermore, neurons of both populations displayed selectivity in their discharge rates to temporal features within a short time-window. Our results suggest that the combination of temporal and rate codes in the auditory cortex provides a possible neural basis for the wide perceptual range of temporal information.

Sounds in the natural environment have complex temporal structures that include both slowly and rapidly changing acoustic transients. In particular, the temporal features of complex communication sounds (such as human speech, animal vocalizations) that convey behaviorally relevant information display a broad variety of acoustic transients that can occur within a few milliseconds or that can span several hundred milliseconds and longer. For example, speech has components that range from slow (<10 Hz) rhythms of syllables and phrases to rapid (>100 Hz) temporal features that can provide cues to a speaker's identity<sup>1</sup>. Neurons in the cortex show sensitivity to temporal manipulations of species-specific communication calls<sup>2-5</sup>. Cortical lesion studies demonstrate the importance of the auditory cortex in the perception of time-varying sounds across a large range of time scales<sup>6-8</sup>. How this wide range of time-varying features is represented by the auditory cortex is still unresolved, as previous studies show that although auditory cortical neurons can exhibit precise onset responses<sup>9</sup>, they still have limitations in their stimulus-synchronized temporal discharge patterns in response to trains of successive acoustic stimulation<sup>10-18</sup>. Whereas the auditory nerve can show phase-locked discharges to pure tones of up to several kilohertz<sup>19</sup> or to the envelope of amplitude modulated (AM) tones at modulation rates above 1 kHz<sup>20</sup>, neurons in the primary auditory cortex (A1) do not typically exhibit stimulus synchronization to more than 100 Hz<sup>10-18,21</sup>. The known response properties of the auditory cortex, therefore, do not adequately explain why the auditory system is capable of resolving temporal differences on a millisecond time scale<sup>22,23</sup>.

There are two issues concerning the apparent discrepancy between the results of cortical neurophysiology and psychophysics. First, neurophysiological studies of the auditory cor-

tex have largely been conducted in the presence of anesthetics, which have suppressive effects on stimulus-synchronized responses in the auditory cortex<sup>24</sup>. However, data from unanesthetized animals are limited. Second, because neural responses in anesthetized auditory cortex are largely phasic, there is much focus in analyzing stimulus-synchronized temporal discharge patterns but less interest in rate coding as a possible way to represent time-varying signals. Here we examined the possibility that rapid acoustic transients may be encoded by non-synchronized discharges. We show that rate representations are indeed an important mechanism in the auditory cortex, especially in encoding fine temporal features.

## RESULTS

The results are based on 94 neurons that were recorded from the auditory cortex of 4 awake marmoset monkeys, a highly vocal primate species<sup>25</sup>. All neurons were tested using sequences of clicks and using sinusoids with temporally asymmetric envelopes (see Methods). The click stimulus protocols were designed to probe the stimulus-synchronizing ability of auditory cortical neurons in awake monkeys. These neurons could be separated into two populations based on their responses to click trains, one with stimulus-synchronized discharges and the other with non-synchronized discharges. The second stimulus protocol tested the sensitivity of these same neurons to rapid acoustic transients within a short time window. We found that both populations of neurons showed selectivity, based on average discharge rate, to rapid acoustic transients. The third stimulus protocol tested the responses of neurons to successive stimuli with embedded temporal asymmetry. We found that neurons could simultaneously represent both temporal aspects of these stimuli.

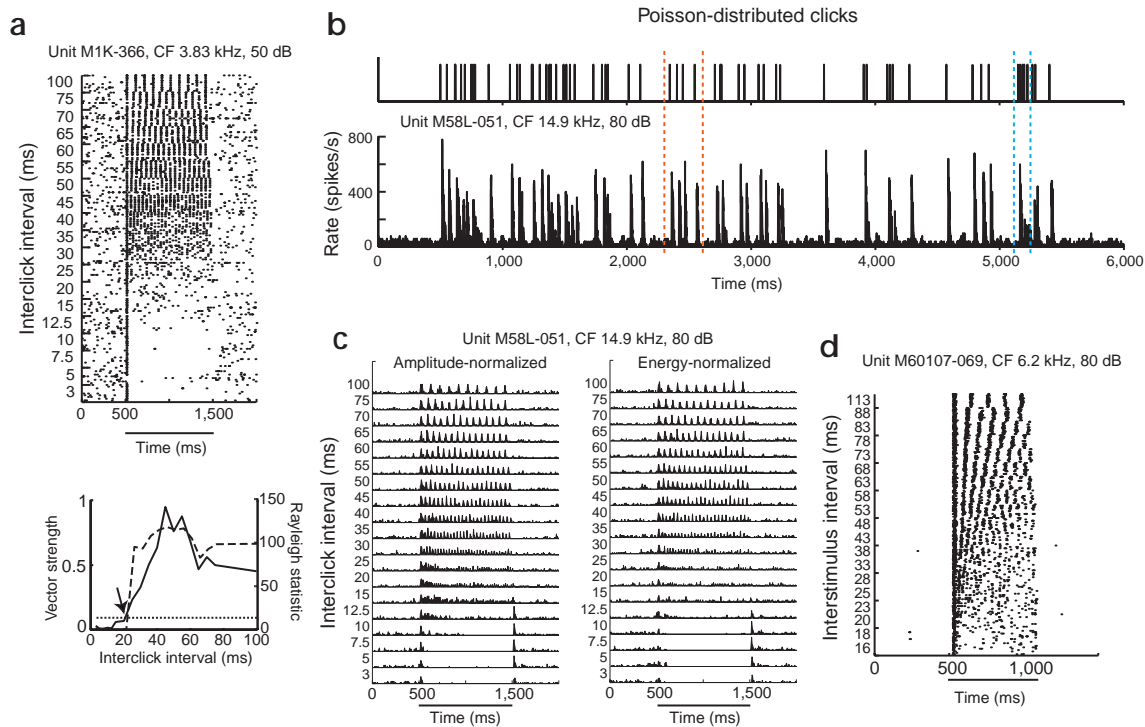


**Fig. 1.** Stimulus-synchronized responses to repetitive acoustic events. (a) Top, stimulus-synchronized responses to click trains, for a representative neuron. Dot rasters from 10 trials at each interclick interval (ICI). Stimulus duration is indicated by the horizontal bar below the time axis. Bottom, dashed line indicates vector strength of the responses to click trains (left ordinate); solid line indicates Rayleigh statistics of stimulus-synchronized activity (right ordinate). Rayleigh statistics greater than horizontal dotted line at 13.8 indicate  $p < 0.001$ . The calculated synchronization boundary is indicated by an arrow. (b) Example of stimulus-synchronized responses to click train stimuli with random ICIs. Time-amplitude waveform of a click train (top) is shown along with the corresponding post-stimulus time histogram (bottom). Bin sizes, 1 ms. Areas within dashed lines indicate portions of the stimulus and response where ICIs were long (red) or short (blue). (c) Comparison between responses to amplitude-normalized (left) and energy-normalized (right) click trains recorded from a typical neuron. (d) An example of synchronized responses to sequences of linear upward frequency-modulated (FM) sweeps. Each FM sweep was centered at the neuron's characteristic frequency (CF) with a width of 0.8 octave and a duration of 12.5 ms.

### Stimulus-synchronized temporal representation

Some neurons showed precise stimulus-synchronized discharges to click trains with long interclick intervals (ICIs; Fig. 1a, top). At 100 ms ICI, the timings of the clicks were explicitly represented by the timing of the discharges, with little adaptation in the strength of the discharges. Shorter ICIs produced correspondingly shorter intervals between bursts of discharges. For ICIs shorter than 15 ms, the response consisted only of an onset to the click train followed by inhibition that lasted for the duration of the stimuli. These observations were quantified by vector strength (VS) and Rayleigh statistics<sup>18,26</sup> (Fig. 1a, bottom). The shortest ICI to which a neuron showed significant stimulus-synchronized activity for all longer ICIs was defined as the synchronization boundary (see Methods) (Fig. 1a, bottom).

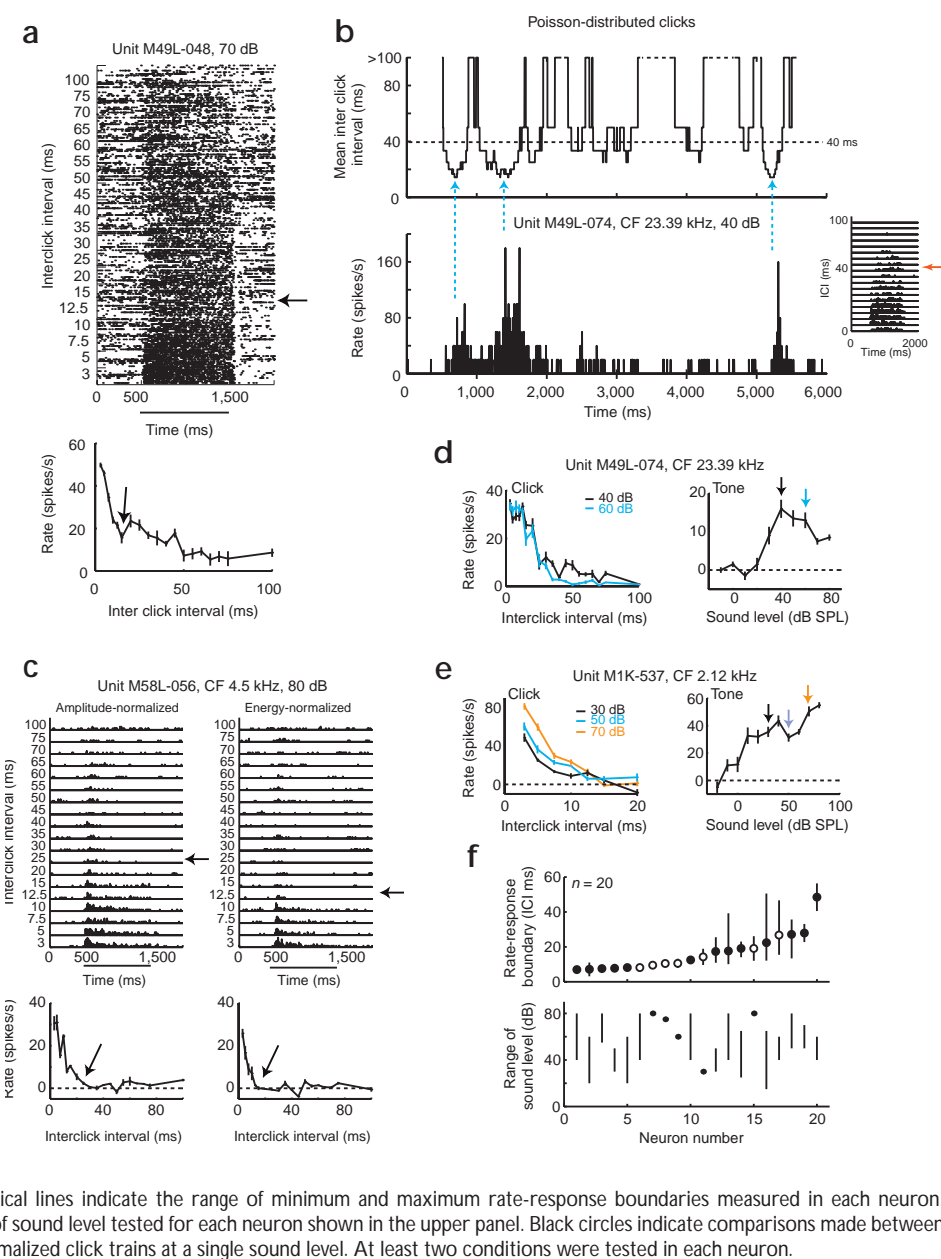
Stimulus-synchronized discharge patterns can also be demonstrated with click trains containing random intervals (Fig. 1b). Clicks that were separated by long intervals were readily resolved by the individual responses (Fig. 1b). Where the clicks were close together, the magnitude of the responses in the post-stimulus time histogram was smaller (Fig. 1b), as predicted by the responses to constant-interval click trains recorded from the same neuron shown in Fig. 1c (left).

Because the click trains in Fig. 1a were amplitude-normalized, click trains with shorter ICIs have greater energy level within a given time period. However, normalizing each click

train to the energy level of the 100 ms ICI click train did not generally affect the pattern of stimulus-synchronized activity. The responses in a representative neuron (Fig. 1c) to amplitude-normalized (left) and energy-normalized (right) click trains showed similar discharge patterns that were significantly synchronized to click trains with ICIs greater than 10 ms. These results indicate that the temporal limitations in this type of cortical neuron were largely determined by the temporal characteristics of the click train stimuli, that is, the ICIs rather than by the overall energy level.

The limited stimulus-synchronized responses of auditory cortical neurons illustrated in Fig. 1a–c can also be shown with sequential stimuli other than click trains. For example, the neuron in Fig. 1d responded to linear frequency-modulated (FM) sweeps but not to most other stimuli tested (including click trains). When the interstimulus interval (ISI) between successive FM sweeps was sufficiently long (>25 ms), we observed neural discharges synchronized to each sweep in the sequence. Neural responses at shorter ISIs (<20 ms) showed strong onset responses followed by weakly driven and non-synchronized discharges. In general, when a neuron exhibited stimulus-synchronized discharge patterns, the limit on its stimulus-synchronizing capacity was similar when determined by click-train stimuli or other sequential stimuli with different spectral characteristics. We refer to these neurons as the synchronized population.

**Fig. 2.** Non-synchronized rate responses to click trains. **(a)** Sustained discharges at short interclick intervals (ICIs) in a representative neuron. Dot rasters (top) and rate functions (bottom) are shown. The calculated rate-response boundary is indicated by arrows. Vertical bars represent standard error of the mean in **(a, c, d, e)**. **(b)** Example of responses to click trains with random ICIs. Top, mean ICI profile (averaged over a moving time window of 200 ms). Mean ICIs longer than 100 ms are truncated in the plot. Bottom, corresponding past stimulus time histogram. Bin sizes, 1 ms. Blue arrows indicate clusters of short ICIs. Right, responses to fixed-interval click trains recorded from the same neuron. A red arrow indicates the calculated rate-response boundary. **(c)** A representative example of rate responses to amplitude-normalized and energy-normalized click trains. Arrows indicate calculated rate-response boundaries. **(d, e)** Left, discharge rates as a function of ICIs measured at different sound levels in two representative neurons. Right, corresponding rate-level functions measured by characteristic frequency tones in the same neuron. Arrows indicate sound levels tested. **(f)** Effects of sound level and energy-normalization analyzed in a group of neurons with non-synchronized responses. Top, black circles indicate mean rate-response boundaries for each neuron over the sound levels tested using only amplitude-normalized clicks. White circles indicate mean rate-response boundaries obtained using both amplitude-normalized and energy-normalized clicks. Units are ordered by their mean rate-response boundaries. Vertical lines indicate the range of minimum and maximum rate-response boundaries measured in each neuron. Bottom, vertical lines indicate ranges of sound level tested for each neuron shown in the upper panel. Black circles indicate comparisons made between amplitude-normalized and energy-normalized click trains at a single sound level. At least two conditions were tested in each neuron.



### Non-synchronized rate representation

Neurons with stimulus-synchronized responses (Fig. 1) cannot fully represent click trains (and likely other sequential stimuli) over the full range of detectable ICIs (or ISIs), particularly at short ICIs, by their limited responses. Another population of neurons, referred to hereafter as the non-synchronized population, had discharge rates inversely proportional to short ICI lengths. In response to rapid clicks (ICIs less than 20 ms), a typical non-synchronized neuron showed prominent and sustained non-synchronized discharges for the stimulus duration (Fig. 2a). An increase in the ICI produced a corresponding decrease in the discharge rate. Discharge rate changed slowly as ICIs lengthened beyond 15 ms. The responses of this type of neuron to click sequences at short ICIs were typically sustained throughout the stimulus duration. The ICI in which the discharge rates no longer

monotonically decreased with increasing ICI is referred to here as the non-synchronized rate-response boundary (Fig. 2a, arrows). This rate-response boundary value indicates the maximum ICI below which perturbations in the ICIs were reflected by changes in the average discharge rate.

As illustrated by Fig. 2a, rate responses of neurons can implicitly represent short ICIs in constant-interval click trains. We also presented click trains with random ICIs to a neuron that showed non-synchronized rate responses (Fig. 2b, right). The neuron showed large increases in discharge rate (Fig. 2b, bottom) following the presence of short intervals (arrows, Fig. 2b, top), but was only weakly responsive when the average ICI was greater than 40 ms.

Because discharge rate generally depends on sound intensity, we verified that the non-synchronized rate response to short ICIs was maintained under energy-normalized stimulus conditions

**Fig. 3.** Population responses to click trains. **(a)** Characterization of two populations of neurons by synchronization and rate-response measures. The horizontal dashed line at 13.8 indicates the statistical significance level of the Rayleigh test ( $p < 0.001$ ). The vertical dashed line indicates a discharge rate ratio of 1.0 (see Methods). White circles indicate neurons classified in the synchronized population ( $n = 36$ ). Crosses indicate neurons classified in the non-synchronized rate-response population ( $n = 50$ ). Black circles indicate neurons with mixed responses ( $n = 8$ ). **(b)** Distribution of synchronization boundaries. **(c)** Distribution of rate-response boundaries. **(d)** Combination of temporal and rate representations of the entire range of tested ICIs. Each curve is the cumulative sum of the histograms representing the neural population in **(b)** or **(c)**, respectively. Dashed line shows the percentage of neurons with synchronization boundaries less than or equal to a given ICI. Solid line shows the percentage of neurons with rate-response boundaries greater than or equal to a given ICI. **(e)** Mean vector strength across the population of synchronized neurons. Vector strength at ICIs below a neuron's synchronization boundary was set to zero. **(f)** Mean discharge rate across the population of non-synchronized neurons. Discharge rates at ICIs above a neuron's rate-response boundary were set to zero. Vertical bars indicate standard error of the mean in **(e, f)**.

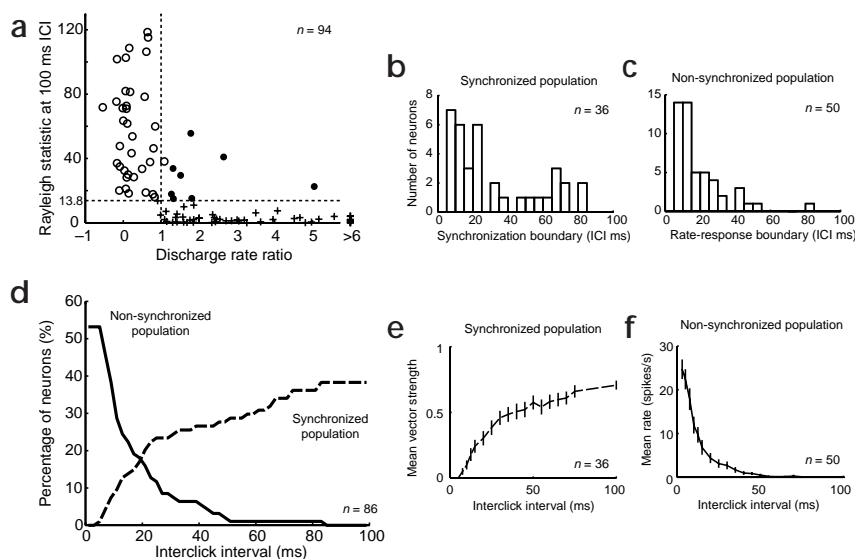


(Fig. 2c). Amplitude-normalized (rate-response boundary, 26.1 ms ICI; Fig. 2c, left) and energy-normalized conditions (rate-response boundary, 12.1 ms; Fig. 2c, right) had similar rate-response profiles. We further verified that the rate-response profile was maintained over different overall sound levels. As an example, the neuron in Fig. 2d had similar rate-response profiles as a function of ICI at both 40 and 60 dB sound pressure level (SPL). In another neuron, the non-synchronized rate responses to click trains, measured at three sound levels (30, 50 and 70 dB SPL), appeared to converge near 15 ms ICI (Fig. 2e). We observed that most neurons tested under different sound-level conditions maintained similar rate-response boundaries (Fig. 2f). In general, changing the sound level of the click trains did not cause non-synchronized neurons to show synchronized activity, nor did it cause stimulus-synchronized neurons to show the type of rate responses illustrated in Fig. 2. As non-synchronized rate-responses were preserved despite the normalized energies of the click trains, rate-responses were most likely due to the temporal features but not the energy level of the stimuli.

#### Population properties and a two-stage mechanism

The stimulus-synchronized and stimulus-non-synchronized populations of neurons can be largely segregated using two response measures, the Rayleigh statistic at 100 ms ICI and a discharge rate ratio of two ICI lengths (Fig. 3a, see Methods). Synchronized neurons (36/94) generally had high Rayleigh statistics and low discharge rate ratios; non-synchronized neurons (50/94) generally had low Rayleigh statistics and high discharge rate ratios. A few neurons (8/94) did not fall into either of these categories. The synchronization boundaries (Fig. 3b) had a median value of 21.3 ms ICI (25–75%, 12.4–54.3 ms). The rate-response boundaries (Fig. 3c) had a median value of 12.9 ms ICI (25–75%, 9.9–23.3 ms). The distributions of characteristic frequency (CF) between the synchronized (0.8–32.3 kHz) and non-synchronized (0.6–26.9 kHz) populations were not significantly different ( $p = 0.21$ , Wilcoxon rank-sum). We found no

correlation between CF and synchronization boundary for the synchronized population ( $r = 0.06$ ) or between CF and rate-response boundary for the non-synchronized population ( $r = -0.05$ ), indicating that both temporal and rate codes were available over a wide frequency range.

At long ICIs, most neurons showed stimulus-synchronized activity (Fig. 3d). The situation was reversed at short ICIs, where the percentage of neurons with non-synchronized rate-responses was much greater than the percentage with synchronized responses. There was a deflection point in the cumulative distribution of the synchronized population near 25 ms because of the denser clustering of synchronization boundaries below that point (Fig. 3b). Synchronized and non-synchronized neurons overlap between 10 to 25 ms ICI with greater than 10% of total samples in each population. Thus, for any ICI tested in this study (3–100 ms), there was always a subpopulation of neurons whose activities reflected the stimulus parameters. Additionally, both mean VS (Fig. 3e) and mean discharge rate (Fig. 3f) averaged over the synchronized and non-synchronized populations, respectively, reflected the trends of the response boundaries of individual neurons. The complementary properties of the two populations of neurons indicate that their combined activities may represent, in a two-stage mechanism, a wide range of temporal intervals. The timing of relatively slowly occurring sequential acoustic events can be explicitly represented by the temporal discharge patterns of the stimulus-synchronized population. Faster rates of acoustic events can be implicitly represented by the average discharge rate of neurons in the non-synchronized population.

#### Dual temporal and rate coding by single neurons

The limit on stimulus-synchronized responses to sequential, click-train stimuli did not reveal, however, whether the neurons in the synchronized population were sensitive to fine temporal features within a resolved acoustic event. To address this, we tested the synchronized population of neurons using ramped

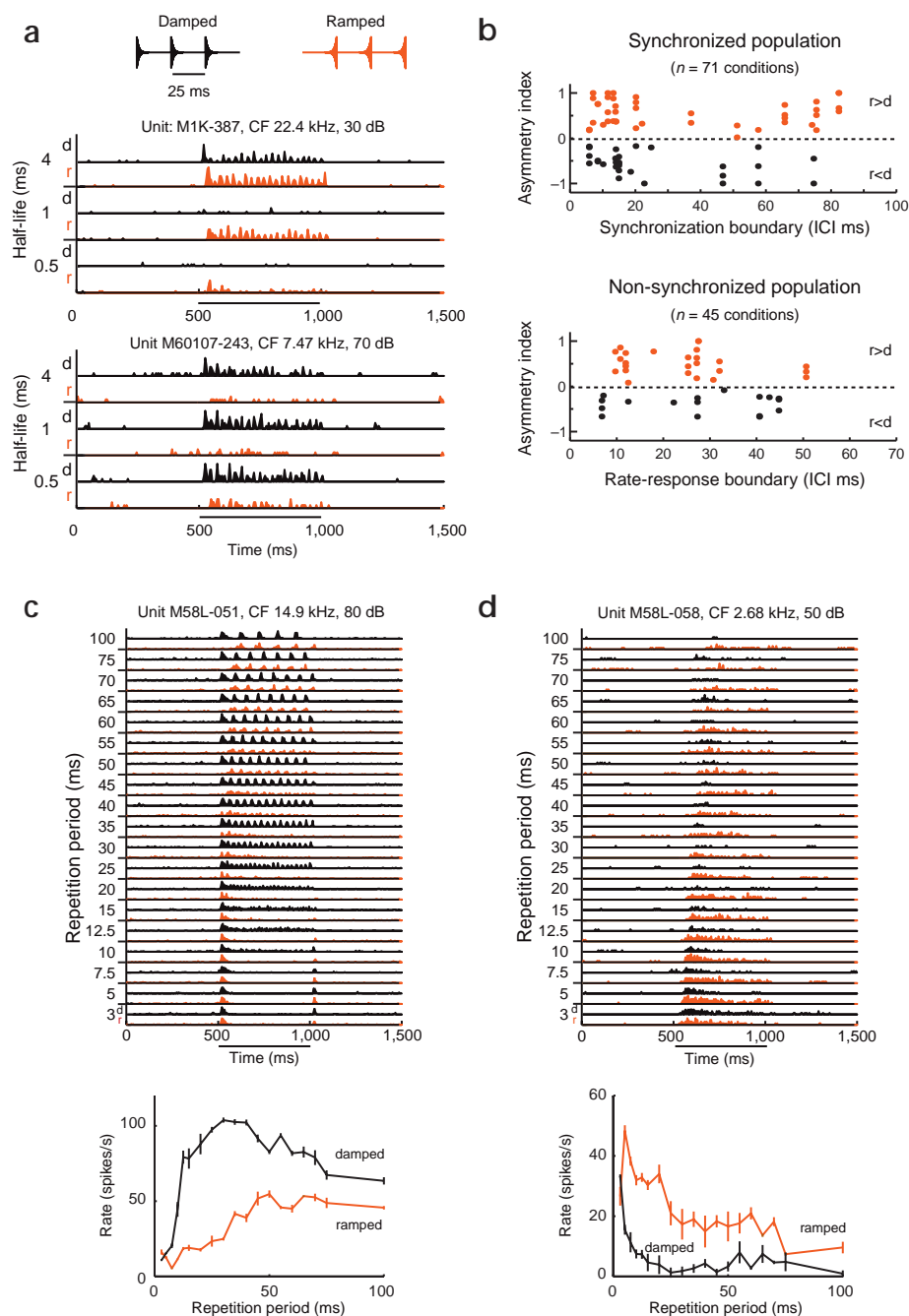


**Fig. 4.** Neural selectivity to temporal asymmetry. **(a)** Top, examples of temporally asymmetric ramped (red) and damped (black) sinusoids. The corresponding responses are colored accordingly. Middle, expression of both stimulus-synchronized responses and selectivity to ramped sinusoids, in a representative neuron. Bottom, stimulus-synchronized responses showing selectivity to damped sinusoids, in a representative neuron. **(b)** Asymmetry indices (see Methods) for neurons in the synchronized and non-synchronized populations. Data points represent statistically significant asymmetry index values calculated at multiple half-life values tested for each neuron. **(c)** Response of a synchronized neuron selective to damped sinusoids across different repetition periods (3–100 ms). Top, post-stimulus time histogram. Bottom, average discharge rate as a function of stimulus repetition period. Both ramped and damped stimuli were presented for each repetition period. Half-life, 4 ms. **(d)** Selectivity of ramped sinusoids in a non-synchronized neuron. The stimuli were the same as those in **(c)**, but the half-life was 1 ms. **(c, d)**, bottom) Vertical bars indicate standard error of the mean.

to temporal asymmetry within a short time window. Asymmetry indices (see Methods) that quantify the selectivity to the ramped and damped sinusoids were not correlated with either the synchronization boundary or the rate-response boundary for the synchronized and non-synchronized populations, respectively (**Fig. 4b**). These results indicate that a neuron's preference to rapid temporal changes within a short time window was largely independent of its response property as defined by sequential stimuli.

When the repetition periods of the ramped and damped stimuli were systematically varied, a neuron could show stimulus-synchronized discharge patterns at long repetition periods and, at the same time, an overall selectivity to temporal asymmetry. In an example neuron (**Fig. 4c**), discharge rates in response to damped sinusoids were consistently higher than discharge rates in response to the ramped sinusoids for almost all repetition periods tested. We also observed stimulus-synchronized neurons selective for ramped stimuli (for example, **Fig. 4a**). Thus, explicit temporal representation of ISIs at coarser time scales can occur simultaneously with a rate-representation of fine temporal features by single neurons.

Selectivity of temporal asymmetry at different repetition periods occurred in non-synchronized neurons as well. In the exam-

and damped sinusoids with temporally asymmetric envelopes<sup>27</sup> (**Fig. 4a**, top). The long-term Fourier magnitude spectra between the ramped and damped sinusoids are identical, as they are time-reversed versions of each other. Psychophysical studies show that the ramped and damped sinusoids can be discriminated by both humans and animals<sup>27,28</sup>, and a neural correlate may exist in auditory cortex<sup>29</sup>.

Neurons in the synchronized population can be selective to the temporal asymmetry within a time window of 25 ms. One representative neuron (**Fig. 4a**, middle) discharged more strongly to the ramped sinusoids than to the damped sinusoids. Another showed the opposite response selectivity (**Fig. 4a**, bottom). Neurons in the non-synchronized population can also be selective

ple illustrated in Fig. 4d, as the repetition period was increased from 3 ms to 20 ms, discharge rates decreased in a manner similar to responses to click train stimuli, while overall responses to ramped sinusoids were stronger than responses to damped sinusoids. These observations suggest that rate representations of two different temporal aspects of stimuli can occur simultaneously in the same neuron in the non-synchronized population.

## DISCUSSION

### Temporal and rate representations

Here we examined the representation of time-varying sounds over a wide time scale by neurons in the auditory cortex of awake primates. Our results provide evidence that the auditory system transforms rapidly changing temporal features into a rate representation at the cortical level that bears no fine structural similarities to the stimuli. Although characteristics of the neurons with stimulus-synchronized discharges have long been studied (for review, see ref. 30), response properties of non-synchronized neurons in auditory cortex have not been previously reported. The existence of these non-synchronized neurons provides a possible means for the auditory cortex to represent rapidly occurring sequences of acoustic events. These observations suggest that perceptual capacity related to fine temporal features (such as roughness) might be due in part to rate representations by cortical neurons.

Additionally, we showed that sensitivity of a cortical neuron to rapid temporal features could be coded alongside the representation of slowly occurring sequential events. These results suggest that an auditory cortical neuron can play multiple roles in encoding different temporal features of a stimulus, and that the auditory cortex can sufficiently encode the wide range of complex, time-varying sounds by a combination of temporal and rate representations, or explicit and implicit mechanisms (Fig. 3d). The overlap between operating ranges of the synchronized and non-synchronized populations of neurons in the auditory cortex provides continuity for representing slow and rapid time-varying features. Although rate coding is widely discussed in the literature on visual cortex<sup>31</sup> and somatosensory cortex<sup>32</sup>, it has not attracted much attention in the literature about the auditory cortex, as there are limited stimulus-driven, sustained discharges to support rate-coding schemes in the auditory cortex of anesthetized animals. Although the proposed two-stage mechanism is largely based on cortical responses to click train stimuli, it can be generalized to other types of time-varying sounds (Figs. 1d, 4c and 4d). It also has direct implications for cortical coding of time-varying signals in other sensory systems.

### Comparison with previous studies

Most previous studies investigating auditory cortical responses to sequential stimuli such as click trains have been conducted in anesthetized animals. Stimulus-synchronization rates reported in the few studies conducted on unanesthetized animals<sup>10,16,17,24</sup> are generally higher than those reported in studies done on anesthetized animals.

Our observations on the synchronized population of auditory cortical neurons are largely consistent with previous observations in unanesthetized animals. Recordings from unanesthetized cat auditory cortex reveal evoked potentials stimulus-synchronized up to 200 Hz<sup>24</sup> (5 ms ICI) and neural discharges up to 300 Hz with a median value between 50 and 100 Hz<sup>10</sup> (10–20 ms ICI). Stimulus-synchronized multi-unit activity in the auditory cortex of awake macaque monkeys occurred up to 300 Hz (3.33 ms ICI) using click trains<sup>17</sup>. In the

auditory cortex of unanesthetized rabbits, 50% recovery of response to the second click in a click pair occurred at ~20 ms<sup>33</sup>. There is nevertheless some—likely small—possibility that our sampling and those of others missed neurons in the auditory cortex with synchronization rates higher than those reported here and elsewhere. It is also possible, however, that neurons in thalamocortical input layers have higher synchronization rates than those in upper cortical layers, where most of our recordings were made. Neurons in upper layers of A1, representing outputs to other cortical fields, process further thalamocortical inputs and outputs of neurons in middle layers. It has been demonstrated by generic compartment models that discharge synchronization to stimulus carrier or envelope can be reduced by dendritic filtering and temporal integration<sup>34</sup>. Moreover, we found that the median synchronization boundary for neurons recorded from the auditory cortex of awake marmosets (Fig. 3) was lower than that determined from anesthetized cats in our previous study<sup>18</sup> using the same set of click train stimuli (marmoset, 21.3 ms; cat, 39.8 ms).

The most striking difference between this and previous studies is the observation of a large percentage of neurons with non-synchronized rate responses (Fig. 2). We describe in a previous study<sup>18</sup> a very small number of neurons recorded in the auditory cortex of anesthetized cats that also exhibit rate responses at short ICIs. However, these responses are generally weak and transient in nature. Neurons in the auditory cortex of awake marmosets, on the other hand, responded to click trains of short ICIs with strong and sustained firings (Fig. 2a). Previous findings show that neurons in the auditory cortex of awake squirrel monkeys show sensitivity in their discharge rates to high modulation frequencies of AM stimuli<sup>16</sup>. Although high-frequency modulations by stimulus components placed away from a neuron's excitatory receptive field may influence the firing rate of a cortical neuron<sup>35</sup>, this is a phenomenon fundamentally different from the rate response to short temporal intervals described in this report. Temporal modulations in our stimuli were created by spectral components centered on a neuron's excitatory receptive field.

### Correlation with psychophysics

The results presented in this study may explain some of the changes in perceptual quality of sounds as the intervals between successive acoustic events vary over time. The number of neurons in the synchronized population decreased as the ICI was shortened, predicting reduced perceptual ability to resolve individual acoustic events at short ISIs. Indeed, the perception of repeated noise bursts is described as discrete when the ISIs are long (>25 ms) and as continuous when they are short (<4 ms)<sup>36</sup>. About 20 ms of separation between a pair of clicks is required for 75% correct judgment of temporal order when the two clicks have different amplitudes<sup>37</sup>. Cortical magnetoencephalographic recordings in humans show that responses to individual clicks in a pair become difficult to resolve when the intervals become shorter than 15–20 ms<sup>38</sup>. Although our data and those cited psychophysical measurements were obtained from different species, several studies show that non-human primates and humans display similar properties in psychophysical measures such as temporal integration functions and temporal modulation transfer functions<sup>39,40</sup>.

Because stimulus-synchronized discharges do not occur at short ISIs, non-synchronized discharges seem to provide a basis for the auditory cortex to differentiate unresolved temporal features. Only a few milliseconds are required for humans to dis-

criminate between pairs of time-reversed click pairs<sup>23,41</sup>, even though they cannot individually resolve the clicks at such a short time scale. Detection thresholds as short as 2 ms are found with sinusoid pairs of different amplitudes<sup>42</sup> or when introducing gaps in noises<sup>22</sup>. In addition, humans can discriminate temporal asymmetry within a short time window introduced by ramped and damped sinusoids<sup>27,43,44</sup>. Stimulus-synchronized responses cannot fully account for such fine perceptual capacity<sup>29</sup>. At sufficiently short intervals, click trains elicit a sensation of pitch equal to the click rate (independent of click polarity) if repetition rates are less than 100 Hz, or equal to the fundamental frequency (dependent on click polarity) for rates greater than 200 Hz<sup>45</sup>. Pitch can arise from stimuli with no frequency components at the perceived pitch frequency<sup>46</sup>, that is, stimuli with a missing fundamental frequency. The lower limit of pitch, defined as the lowest repetition rate that evokes a sensation of pitch, is about 30 Hz<sup>47</sup>, which is near the 25-ms ICI deflection point in the cumulative distribution of synchronization boundary of the stimulus-synchronized population (Fig. 3d).

Findings of our study suggest that a combination of temporal and rate codes in the auditory cortex, representing slowly and rapidly occurring acoustic events, respectively, may serve as the neural basis for the wide perceptual range of temporal information.

#### METHODS

**Recording procedure.** Marmoset monkeys (*Callithrix jacchus jacchus*) were adapted to sit quietly in a semi-restraint device within a sound-proof chamber (Industrial Acoustics, Bronx, New York). We developed a chronic recording preparation to laterally approach the auditory cortex<sup>29</sup>, which lies largely on the surface of the superior temporal gyrus in the marmoset<sup>4,48,49</sup>. Action potentials of single neurons were recorded using tungsten microelectrodes (A-M Systems, Carlsborg, Washington) with impedances of 2–5 M $\Omega$  (at 1000 Hz) and detected by a template-based spike discriminator (MSD, Alpha Omega Engineering, Nazareth, Israel). The data presented were mainly obtained from the primary auditory cortex (A1) and may have included a few neurons from the immediately adjacent areas. The location of the primary auditory cortex was determined by its tonotopic organization, its relationship to the lateral belt area (which was more responsive to noises than tones<sup>50</sup>), and the response properties of its neurons (which have short latencies and are highly responsive to tones). Single neurons were encountered at all cortical layers, but most recorded data were from upper layers, judging by the depths and response characteristics. All experimental procedures were approved by the Johns Hopkins University Animal Use and Care Committee.

**Acoustic stimuli.** Acoustic signals were generated digitally and delivered in free-field through a speaker located approximately 1 m in front of the animal. Once a neuron was isolated and its basic response properties (such as CF, latency and rate-level characteristics) were determined, other stimulus protocols were executed in randomized blocks for 5 or 10 repetitions. Intertrial intervals were at least 1.5 s long. Unless indicated, sound intensity was typically set at the peak of the neuron's rate-level function if it was non-monotonic or 10–30 dB above the threshold if it was monotonic.

We used three sets of acoustic stimuli. The first set were wide- and narrow-band click trains with constant interclick intervals (ICI) ranging from 3 to 100 ms. Wide-band clicks were 0.1-ms rectangular pulses. Because only a small percentage of neurons in the unanesthetized auditory cortex were responsive to this type of stimulus, we also used narrow-band clicks, sinusoids at a neuron's CF that were amplitude-modulated by a Gaussian envelope<sup>18</sup>. The bandwidths were controlled by the standard deviation parameter,  $\sigma$ , ranging from 0.1 to 0.4. A larger  $\sigma$  value gives a wider temporal envelope and a narrower spectral peak. An optimal  $\sigma$  value was chosen for each neuron. We also tested some neurons with five-second-long click trains of random ICIs based on a modified Poisson distribution ( $\lambda = 70$  ms) with a dead time

of 3 ms. Fifty repetitions of the same sequence were delivered for each random-ICI click train.

The second set of stimuli, ramped and damped sinusoids<sup>27</sup> (Fig. 4a, top), were generated by modulating a sinusoidal carrier at a neuron's CF with an exponential function. The half-life of the exponential function, ranging from 0.5 to 32 ms, determined the time course of the amplitude modulation. A smaller half-life corresponded to a more rapid rising (ramped) or falling (damped) envelope. Each stimulus was repeated every 25 ms to a total duration of 500 ms. The sinusoidal carrier was continuous in phase throughout the entire duration.

The third set of stimuli were ramped and damped sinusoids with repetition periods that were systematically changed from 3 to 100 ms in the same steps as used for the click train ICIs, resulting in a set of sequential stimuli with embedded temporal asymmetries.

**Data analysis.** Data were analyzed using custom software implemented in Matlab (Mathworks, Natick, Massachusetts). Average discharge rates were calculated over the entire stimulus duration and spontaneous discharge rates were subtracted. Of 217 neurons tested in 4 animals, 190 neurons responded in some manner to the click stimuli. Of these 190 neurons, 86 (45%) showed clearly defined synchronized responses or non-synchronized rate responses. Synchronized and non-synchronized neurons seemed to be intermingled and were encountered throughout different recording sites and depths. Eight additional neurons (4%) showed mixed responses (Fig. 3a). The remaining neurons showed varying degrees of responsiveness to click-train stimuli, but had no significant stimulus-synchronized discharges at an ICI of 100 ms. Among them, approximately 14% (26/190) of neurons showed monotonically increasing discharges rates with increasing ICI. A smaller percentage, 7% (14/190), showed band-passed rate responses. Another 6% (12/190) showed only inhibited responses. The remaining 23% (44/190) did not seem to have definite ICI-dependent responses. Neurons in the last two groups did not seem to be optimally driven by the click train stimuli used in this study.

Stimulus-synchronized temporal patterns were quantified by VS and statistically assessed with a Rayleigh test<sup>18,26</sup>. To ensure sustained synchronized responses, two values of the Rayleigh statistic were calculated for each ICI using the first and second halves of the response, and the minimum of the two statistics was used in the determination. Onset responses (<100 ms) were excluded from the calculation of the VS. For neurons in the synchronized population, a synchronization boundary was calculated from the Rayleigh statistic versus ICI curve with a two-step analysis. First, an estimate of the synchronization boundary was obtained using a threshold value of 13.8 ( $p < 0.001$ , Rayleigh)<sup>26</sup>. A linear interpolation between the estimated boundary ICI and the next tested shorter ICI were used to obtain the synchronization boundary, that is, the ICI where the Rayleigh threshold was crossed.

For neurons in the non-synchronized population, an estimate of rate-response boundary was obtained as the minimum ICI where the discharge rate was not significantly different from either the spontaneous rate or the rate at the preceding, shorter ICI ( $p > 0.05$ , Wilcoxon rank-sum). The rate-response boundary was calculated to be where a linear curve fit, based on discharge rates from 3 ms ICI to the estimated boundary, crossed the level of discharge rate corresponding to the estimated boundary.

A discharge rate ratio was used to further quantify the separation of the two populations of neurons based on their responses to click trains (Fig. 3a). It was defined as the maximum discharge rate occurring at ICIs less than 5 ms divided by the maximum discharge rate occurring at ICIs greater than 30 ms. Neurons in the non-synchronized population typically had stronger discharges at short ICIs than at the longer ones. Consequently, their discharge rate ratios were generally greater than one. Conversely, neurons from the synchronized population tended to have weaker discharges at short ICIs, and therefore, their discharge rate ratios were typically less than one or less than zero if they were inhibited (for example, Fig. 1a).

To quantify the asymmetry preference of a cortical neuron to ramped or damped sinusoids, we defined an asymmetry index ( $I$ ) at each half-life value of the stimulus as follows:  $I = (R_r - R_d)/(R_r + R_d)$ , where  $R_r$  and  $R_d$  are the discharge rates to the ramped and damped sinusoids, respectively. Statistical significance of the asymmetry index at each half-life, on a trial-by-trial basis, was assessed using a Wilcoxon rank-sum test. Non-significant ( $p > 0.05$ ) asymmetry index values were set to zero.

**ACKNOWLEDGEMENTS**

The authors thank E. Bartlett and S. Kadia for helpful comments on the manuscript and A. Pistorio for assistance with animal training. This work was supported by NIH Grant DC03180 and by a Presidential Early Career Award for Scientists and Engineers (X. Wang).

RECEIVED 23 MAY; ACCEPTED 13 SEPTEMBER 2001

1. Rosen, S. Temporal information in speech: acoustic, auditory and linguistic aspects. *Phil. Trans. R. Soc. Lond. B Biol. Sci.* **336**, 367–373 (1992).
2. Margoliash, D. Acoustic parameters underlying the responses of song-specific neurons in the white-crowned sparrow. *J. Neurosci.* **3**, 1039–1057 (1983).
3. Doupe, A. J. & Konishi, M. Song-selective auditory circuits in the vocal control system of the zebra finch. *Proc. Natl. Acad. Sci. USA* **88**, 11339–11343 (1991).
4. Wang, X., Merzenich, M. M., Beitel, R. & Schreiner, C. E. Representation of a species-specific vocalization in the primary auditory cortex of the common marmoset: temporal and spectral characteristics. *J. Neurophysiol.* **74**, 2685–2706 (1995).
5. Esser, K.-H., Condon, C. J., Suga, N. & Kanwal, J. S. Syntax processing by auditory cortical neurons in the FM-FM area of the mustached bat *Pteronotus parnellii*. *Proc. Natl. Acad. Sci. USA* **94**, 14019–14024 (1997).
6. Whitfield, I. C. Auditory cortex and the pitch of complex tones. *J. Acoust. Soc. Am.* **67**, 644–647 (1980).
7. Heffner, H. E. & Heffner, R. S. Effect of unilateral and bilateral auditory cortex lesions on the discrimination of vocalizations by Japanese macaques. *J. Neurophysiol.* **56**, 683–701 (1986).
8. Zatorre, R. J. Pitch perception of complex tones and human temporal-lobe function. *J. Acoust. Soc. Am.* **84**, 566–572 (1988).
9. Heil, P. Auditory cortical onset responses revisited. I. First-spike timing. *J. Neurophysiol.* **77**, 2616–2641 (1997).
10. de Ribaupierre, F., Goldstein, M. H. Jr. & Yeni-Komshian, G. Cortical coding of repetitive acoustic pulses. *Brain Res.* **48**, 205–225 (1972).
11. Eggermont, J. J. Rate and synchronization measures of periodicity coding in cat primary auditory cortex. *Hear. Res.* **56**, 153–167 (1991).
12. Cheung, S. W. *et al.* Auditory cortical neuron response differences under isoflurane versus pentobarbital anesthesia. *Hear. Res.* **156**, 115–127 (2001).
13. Creutzfeldt, O., Hellweg, F.-C. & Schreiner, C. Thalamocortical transformation of responses to complex auditory stimuli. *Exp. Brain Res.* **39**, 87–104 (1980).
14. Phillips, D. P., Hall, S. E. & Hollett, J. L. Repetition rate and signal level effects on neuronal responses to brief tone pulses in cat auditory cortex. *J. Acoust. Soc. Am.* **85**, 2537–2549 (1989).
15. Gaese, B. H. & Ostwald, J. Temporal coding of amplitude and frequency modulation in the rat auditory cortex. *Eur. J. Neurosci.* **7**, 438–450 (1995).
16. Bieser, A. & Müller-Preuss, P. Auditory responsive cortex in the squirrel monkey: neural responses to amplitude-modulated sounds. *Exp. Brain Res.* **108**, 273–284 (1996).
17. Steinschneider, M., Reser, D. H., Fishman, Y. I., Schroeder, C. E. & Arezzo, J. C. Click train encoding in primary auditory cortex of the awake monkey: evidence for two mechanisms subserving pitch perception. *J. Acoust. Soc. Am.* **104**, 2935–2955 (1998).
18. Lu, T. & Wang, X. Temporal discharge patterns evoked by rapid sequences of wide- and narrowband clicks in the primary auditory cortex of cat. *J. Neurophysiol.* **84**, 236–246 (2000).
19. Johnson, D. H. The relationship between spike rate and synchrony in responses of auditory-nerve fibers to single tones. *J. Acoust. Soc. Am.* **68**, 1115–1122 (1980).
20. Joris, P. X. & Yin, T. C. T. Responses to amplitude-modulated tones in the auditory nerve of the cat. *J. Acoust. Soc. Am.* **91**, 215–232 (1992).
21. Kilgard, M. P. & Merzenich, M. M. Plasticity of temporal information processing in the primary auditory cortex. *Nat. Neurosci.* **1**, 727–731 (1998).
22. Plomp, R. Rate of decay of auditory sensation. *J. Acoust. Soc. Am.* **36**, 277–282 (1964).
23. Ronken, D. A. Monaural detection of a phase difference between clicks. *J. Acoust. Soc. Am.* **47**, 1091–1099 (1970).
24. Goldstein, M. H. Jr., Kiang, N. Y.-S. & Brown, R. M. Response of the auditory cortex to repetitive acoustic stimuli. *J. Acoust. Soc. Am.* **31**, 356–364 (1959).
25. Wang, X. On cortical coding of vocal communication sounds in primates. *Proc. Natl. Acad. Sci. USA* **97**, 11843–11849 (2000).
26. Mardia, K. V. & Jupp, P. E. *Directional statistics* (John Wiley and Sons, New York, 2000).
27. Patterson, R. D. The sound of a sinusoid: spectral models. *J. Acoust. Soc. Am.* **96**, 1409–1418 (1994).
28. Fay, R. R., Chronopoulos, M. & Patterson, R. D. The sound of a sinusoid: perception and neural representations in the goldfish (*carassius auratus*). *Audit. Neurosci.* **2**, 377–392 (1996).
29. Lu, T., Liang, L. & Wang, X. Neural representations of temporally asymmetric stimuli in the auditory cortex of awake primates. *J. Neurophysiol.* **85**, 2364–2380 (2001).
30. Langner, G. Periodicity coding in the auditory system. *Hear. Res.* **60**, 115–142 (1992).
31. Shadlen, M. N. & Newsome, W. T. Noise, neural codes and cortical organization. *Curr. Opin. Neurobiol.* **4**, 569–579 (1994).
32. Ahissar, E., Sosnik, R. & Haidarliu, S. Transformation from temporal to rate coding in a somatosensory thalamocortical pathway. *Nature* **406**, 302–306 (2000).
33. Fitzpatrick, D. C., Kuwada, S., Kim, D. O., Parham, K. & Batra, R. Responses of neurons to click-pairs as simulated echoes: auditory nerve to auditory cortex. *J. Acoust. Soc. Am.* **106**, 3460–3472 (1999).
34. Wang, X. & Sachs, M. B. Transformation of temporal discharge patterns in a ventral cochlear nucleus stellate cell model: implications for physiological mechanisms. *J. Neurophysiol.* **73**, 1600–1616 (1995).
35. Schulze, H. & Langner, G. Periodicity coding in the primary auditory cortex of the Mongolian gerbil (*Meriones unguiculatus*): two different coding strategies for pitch and rhythm? *J. Comp. Physiol. A* **181**, 651–663 (1997).
36. Miller, G. A. & Taylor, W. G. The perception of repeated bursts of noise. *J. Acoust. Soc. Am.* **20**, 171–182 (1948).
37. Hirsh, I. J. Auditory perception of temporal order. *J. Acoust. Soc. Am.* **31**, 759–767 (1959).
38. Joliot, M., Ribary, U. & Llinas, R. Human oscillatory brain activity near 40 Hz coexists with cognitive temporal binding. *Proc. Natl. Acad. Sci. USA* **91**, 11748–11751 (1994).
39. Brown, C. H. & Maloney, C. G. Temporal integration in two species of old world monkeys: blue monkeys (*Cercopithecus mitis*) and grey-cheeked mangabeys (*Cercocebus albigena*). *J. Acoust. Soc. Am.* **79**, 1058–1064, 4 (1986).
40. Moody, D. B. Detection and discrimination of amplitude-modulated signals by macaque monkeys. *J. Acoust. Soc. Am.* **95**, 3499–3510 (1994).
41. Resnick, S. B. & Feth, L. L. Discriminability of time-reversed click pairs: intensity effects. *J. Acoust. Soc. Am.* **57**, 1493–1499 (1975).
42. Green, D. M. Temporal acuity as a function of frequency. *J. Acoust. Soc. Am.* **54**, 373–379 (1973).
43. Patterson, R. D. The sound of a sinusoid: time-interval models. *J. Acoust. Soc. Am.* **96**, 1419–1428 (1994).
44. Akeroyd, M. A. & Patterson, R. D. A comparison of detection and discrimination of temporal asymmetry in amplitude modulation. *J. Acoust. Soc. Am.* **101**, 430–439 (1997).
45. Flanagan, J. L. & Guttman, N. On the pitch of periodic pulses. *J. Acoust. Soc. Am.* **32**, 1308–1319 (1960).
46. Schouten, J. F., Ritsma, R. J. & Cardozo, B. L. Pitch of the residue. *J. Acoust. Soc. Am.* **34**, 1418–1424 (1962).
47. Krumbholz, K., Patterson, R. D. & Pressnitzer, D. The lower limit of pitch as determined by rate discrimination. *J. Acoust. Soc. Am.* **108**, 1170–1180 (2000).
48. Aitkin, L. M., Merzenich, M. M., Irvine, D. R., Clarey, J. C. & Nelson, J. E. Frequency representation in auditory cortex of the common marmoset (*Callithrix jacchus jacchus*). *J. Comp. Neurol.* **252**, 175–185 (1986).
49. Aitkin, L. & Park, V. Audition and the auditory pathway of a vocal new world primate, the common marmoset. *Prog. Neurobiol.* **41**, 345–367 (1993).
50. Rauschecker, J. P., Tian, B. & Hauser, M. Processing of complex sounds in the macaque nonprimary auditory cortex. *Science* **268**, 111–114 (1995).